Journal of
Mechanics of
Materials and Structures

A SIMPLIFIED STRAIN GRADIENT KIRCHHOFF ROD MODEL AND ITS APPLICATIONS ON MICROSPRINGS AND MICROCOLUMNS

Jun Hong, Gongye Zhang, Xiao Wang and Changwen Mi

Volume 15, No. 2 March 2020

msp

JOURNAL OF MECHANICS OF MATERIALS AND STRUCTURES
Vol. 15, No. 2, 2020
dx.doi.org/10.2140/jomms.2020.15.203

A SIMPLIFIED STRAIN GRADIENT KIRCHHOFF ROD MODEL AND ITS APPLICATIONS ON MICROSPRINGS AND MICROCOLUMNS

JUN HONG, GONGYE ZHANG, XIAO WANG AND CHANGWEN MI

The equilibrium equations and boundary conditions of elastic Kirchhoff rods are presented within the theoretical framework of the simplified strain gradient theory. The newly developed Cosserat rod model contains only one intrinsic material length squared parameter to account for the effects of microstructures. Applications of the theory are also presented in this paper. Examples include the equilibrium analysis of a microspring and the buckling behavior of a microcolumn. The first application focuses on estimating the restoring force of a microspring that is deformed from an originally straight rod with uniform cross-sectional area. Semianalytical results show that the restoring force of the microspring predicted by the new strain gradient rod model is always larger than that of its classical counterpart. The restoring force is found to increase with both the intrinsic material length squared parameter and the rod radius. For the stability analysis of a microcolumn, an analytical expression is derived for the critical buckling load. It is found that the critical force predicted by the developed nonclassical Kirchhoff rod model depends linearly on the intrinsic material length squared parameter, quantitatively indicating the significance of strain gradient effects.

1. Introduction

In microelectromechanical and nanoelectromechanical systems, thin elastic rods are widely used. Examples include micro and nanosprings, medical robots and DNA mechanics [Westcott et al. 1995; McIlroy et al. 2001; Seto et al. 2001; Eslami-Mossallam and Ejtehadi 2009; Burgner-Kahrs et al. 2015; Liangruksa et al. 2017]. Since the characteristic length of these structures is at the micro or even nanoscale, the effects of microstructures on the mechanical behavior of thin rods become increasingly important. For these cases, the classical Kirchhoff rod theory becomes inadequate due to its absence of any intrinsic material parameters. To address this issue, new models need to be developed so that microstructure-dependent material parameters can be taken into account.

In the last four decades, several higher-order elasticity theories have been applied in order to develop nonclassical rod models. Lembo rederived the equilibrium equations of a Kirchhoff rod by employing the nonlocal continuum theory suggested by Eringen [Lembo 2016; Eringen 1983]. The nonlocal integral elasticity theory has been employed by Zhu and Li [2017] in order to analyze the longitudinal and torsional vibrations of size-dependent rods. By the use of Cosserat theory [Lakes 2018], Liu and Wang [2009] developed the equations of motion for a very thin rod. The motion of the rod is formulated in terms of a reference (Cosserat) curve and three orthonormal vectors. Based on a potential energy method, Steigmann [2012] proposed a new theory on fiber-reinforced composites subjected to stretching, bending and twisting. By incorporating the effects of surface tension and surface elasticity [Gurtin and

Gongye Zhang and Changwen Mi are the corresponding authors.
Keywords: simplified strain gradient theory, Kirchhoff rod, microstructural effect, microspring, microcolumn.

Murdoch 1975; Gurtin and Murdoch 1978], Wang et al. [2010] developed a nonclassical rod model and investigated the surface effects of nanosized springs. Employing a microelasticity theory characterized by two additional constitutive parameters, Lazopoulos and Lazopoulos [2010] analyzed the bending and buckling of a thin strain gradient elastic beam.

The simplified strain gradient elasticity theory (SSGET) was developed by Altan and Aifantis [1997]. This theory is also known as the dipolar gradient elasticity theory [Gourgiotis and Georgiadis 2009]. The SSGET model was simplified from the original strain gradient elasticity theory that contains a total number of sixteen intrinsic material parameters [Mindlin 1964]. It can also be reduced from the second form of Mindlin's strain gradient elasticity theory, in which still five additional material parameters are required [Mindlin and Eshel 1968; Polizzotto 2003]. These strain gradient models are relatively more difficult to be applied in engineering practice because of their large number of material parameters [Mindlin and Eshel 1968; Lam et al. 2003; Ansari et al. 2014; Lurie and Solyaev 2018]. In contrast, only a single material parameter is contained in the SSGET version. For this reason, the SSGET framework has been applied to successfully solve many fundamental mechanical problems such as beams [Lazopoulos 2003; Ansari et al. 2012; Chen et al. 2019], plates [Lazopoulos 2004; Papargyri-Beskou and Beskos 2008], shells [Papargyri-Beskou and Beskos 2009; Gao et al. 2009], inclusions [Gao and Ma 2009; 2010] and many other microstructured solids [Gourgiotis and Georgiadis 2009; Georgiadis et al. 2004; Polizzotto 2012].

Couple stress theory has also played a role in rod mechanics. Zhang [2010] proposed a nonclassical Kirchhoff rod model using the classical couple stress theory. Recently, Zhang and Gao [2019] developed a nonclassical Kirchhoff rod model based on a modified couple stress theory [Yang et al. 2002; Park and Gao 2008; Ansari et al. 2015]. Both the governing equations and boundary conditions were derived. Moreover, only one material length scale parameter was used to describe the effects of couple stress. However, although the modified couple stress theory can be reduced from some alternative forms of Mindlin's strain gradient elasticity theory [Mindlin and Eshel 1968; Polizzotto 2017; Norouzzadeh et al. 2018a; 2018b], the couple stress and the simplified strain gradient theories were in nature proposed for describing the rotational and the first-order strain gradient effects, respectively. As a result, there is still a call upon a rod model within the context of the SSGET, such that the effects of strain gradient in Kirchhoff rods can be better evaluated. The present work aims to fill this gap by developing a microstructure-dependent SSGET model for Kirchhoff rods.

In this paper, a nonclassical Kirchhoff rod model is developed based on the SSGET model and the principle of minimum total potential energy, featuring only one additional material constant to account for the strain gradient effects. Based on the authors' knowledge, within the context of SSGET theory, no model that is able to simultaneously accounting for stretching, twisting, and bending deformations has been proposed for an elastic Kirchhoff rod.

This paper is structured as follows. Section 2 presents the SSGET-based theoretical formulation for Kirchhoff rods under the influence of microstructural effects. Both the nonclassical equilibrium equations and boundary conditions are analytically derived. They reduce to the classical Kirchhoff rod model when microstructure-dependent effects are ignored. To illustrate the applications of the proposed SSGET rod model, in Section 3, two examples are provided. The first of which calculates the restoring force in a helical microspring that is deformed from an originally straight rod with uniform cross-section. The second example performs a buckling analysis for a microcolumn. Finally, in Section 4, conclusions are drawn.

2. Theoretical framework

Within the context of the simplified strain gradient elasticity theory [Altan and Aifantis 1997; Gao and Park 2007], the constitutive relations can be written as

$$\sigma_{ij} = \tau_{ij} - \mu_{ijk,k} = (1 - c\nabla^2)\,\tau_{ij}, \tag{1a}$$

$$\tau_{ij} = \frac{E}{1+v}\left(\varepsilon_{ij} + \frac{v}{1-2v}\varepsilon_{kk}\,\delta_{ij}\right) = \tau_{ji}, \tag{1b}$$

$$\mu_{ijk} = c\tau_{ij,k} = \mu_{jik}, \tag{1c}$$

where σ_{ij}, τ_{ij}, and μ_{ijk} are, respectively, the components of total stress, Cauchy stress, and double stress. The symbol δ_{ij} is the Kronecker delta, c is the simplified strain gradient coefficient having the dimension of length squared, E is Young's modulus, v is Poisson's ratio, and ∇^2 denotes the Laplacian operator. It is noted that Equations (1a)–(1c) serve as the constitutive relations for a Kirchhoff rod (Figure 1), featuring one additional constitutive coefficient accounting for strain gradient effects. The components of the infinitesimal strain tensor ε_{ij} can be shown to be [Zhang and Gao 2019; Dill 1992]

$$\varepsilon_{11} = -v\varepsilon + v(\kappa_2 - \kappa_2^0)\,X - v(\kappa_1 - \kappa_1^0)Y, \tag{2a}$$

$$\varepsilon_{12} = 0, \tag{2b}$$

$$\varepsilon_{22} = -v\varepsilon + v(\kappa_2 - \kappa_2^0)X - v(\kappa_1 - \kappa_1^0)Y, \tag{2c}$$

$$\varepsilon_{13} = \frac{1}{2}\left[\frac{\partial x_{01}}{\partial S} - \kappa_3^0 x_{02} + \kappa_2^0 x_{03} - \theta_2 - (\kappa_3 - \kappa_3^0)Y + (\kappa_3 - \kappa_3^0)\frac{\partial \varphi}{\partial X}\right], \tag{2d}$$

$$\varepsilon_{23} = \frac{1}{2}\left[\frac{\partial x_{02}}{\partial S} + \kappa_3^0 x_{01} - \kappa_1^0 x_{03} + \theta_1 + (\kappa_3 - \kappa_3^0)X + (\kappa_3 - \kappa_3^0)\frac{\partial \varphi}{\partial Y}\right], \tag{2e}$$

$$\varepsilon_{33} = \frac{\partial x_{03}}{\partial S} - \kappa_2^0 x_{01} + \kappa_1^0 x_{02} - (\kappa_2 - \kappa_2^0)X + (\kappa_1 - \kappa_1^0)Y, \tag{2f}$$

where (X, Y, S) are the material coordinates forming a curvilinear coordinate system $X^i(X_\alpha, S)$ originated at point P, i.e., $X_1 = X$, $X_2 = Y$ and $X_3 = S$, as shown in Figure 1. It should be noted that, although the strain components given in (2a)–(2f) are only applicable to rods subjected to infinitesimal strains. Nonetheless, finite rotations are allowed, as discussed in more details in [Dill 1992]. The components of the extra displacement $\boldsymbol{x}_0$ are given by

$$\boldsymbol{x}_0(S, t) = \boldsymbol{r}(S, t) - \boldsymbol{R}(S). \tag{3}$$

In addition, θ_1 and θ_2 are components of the small rotation vector $\boldsymbol{\theta}$, κ_i^0 are components of the curvature at the material point, and κ_i represent the components of curvature in the deformed rod. These two curvatures can respectively be defined by [Dill 1992; Coleman et al. 1993]

$$\frac{\partial \boldsymbol{d}_i}{\partial S} = \boldsymbol{\kappa}^0 \times \boldsymbol{d}_i, \tag{4a}$$

$$\frac{\partial \boldsymbol{e}_i}{\partial S} = \boldsymbol{\kappa} \times \boldsymbol{e}_i, \tag{4b}$$

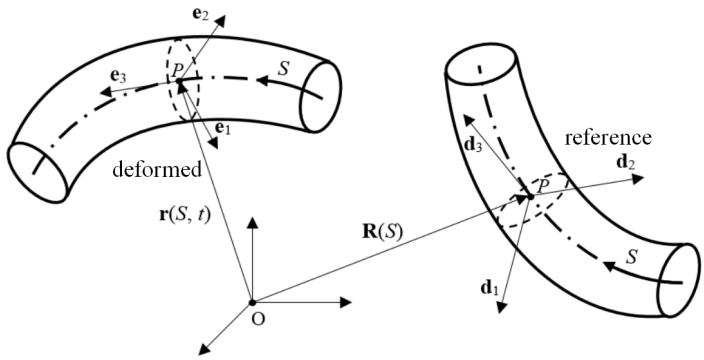

Figure 1. Geometry of a Krichhoff rod: the deformed and the reference configurations.

where $\varepsilon = \partial x_{03}/\partial S - \kappa_2^0 x_{01} + \kappa_1^0 x_{02}$ represents the extension of the centroidal axis along the S direction [Zhang and Gao 2019]. The warping function $\varphi(X, Y)$ describes the torsion of the rod and depends on the cross-sectional shape.

Note that here and throughout this paper, the summation convention and the standard index notation are assumed. Unless otherwise indicated, the Greek indices run from 1 to 2 and the Latin ones range from 1 to 3.

From (1b) and (2a)–(2f), the components of Cauchy stress tensor in the Kirchhoff rod can be derived:

$$\tau_{13} = G\left[\frac{\partial x_{01}}{\partial S} - \kappa_3^0 x_{02} + \kappa_2^0 x_{03} - \theta_2 - (\kappa_3 - \kappa_3^0)Y + (\kappa_3 - \kappa_3^0)\frac{\partial \varphi}{\partial X}\right], \tag{5a}$$

$$\tau_{23} = G\left[\frac{\partial x_{02}}{\partial S} + \kappa_3^0 x_{01} - \kappa_1^0 x_{03} + \theta_1 + (\kappa_3 - \kappa_3^0)X + (\kappa_3 - \kappa_3^0)\frac{\partial \varphi}{\partial Y}\right], \tag{5b}$$

$$\tau_{33} = E\left[\frac{\partial x_{03}}{\partial S} - \kappa_2^0 x_{01} + \kappa_1^0 x_{02} - (\kappa_2 - \kappa_2^0)X + (\kappa_1 - \kappa_1^0)Y\right], \tag{5c}$$

$$\tau_{11} = \tau_{22} = \tau_{12} = 0, \tag{5d}$$

where G is the shear modulus of elasticity, i.e., $G = E/2(1+\upsilon)$. Substituting (5a)–(5d) into (1a) then gives the components of the total stress tensor

$$\sigma_{13} = (1 - c\nabla^2)G\left[\frac{\partial x_{01}}{\partial S} - \kappa_3^0 x_{02} + \kappa_2^0 x_{03} - \theta_2 - (\kappa_3 - \kappa_3^0)Y + (\kappa_3 - \kappa_3^0)\frac{\partial \varphi}{\partial X}\right], \tag{6a}$$

$$\sigma_{23} = (1 - c\nabla^2)G\left[\frac{\partial x_{02}}{\partial S} + \kappa_3^0 x_{01} - \kappa_1^0 x_{03} + \theta_1 + (\kappa_3 - \kappa_3^0)X + (\kappa_3 - \kappa_3^0)\frac{\partial \varphi}{\partial Y}\right], \tag{6b}$$

$$\sigma_{33} = (1 - c\nabla^2)E\left[\frac{\partial x_{03}}{\partial S} - \kappa_2^0 x_{01} + \kappa_1^0 x_{02} - (\kappa_2 - \kappa_2^0)X + (\kappa_1 - \kappa_1^0)Y\right], \tag{6c}$$

$$\sigma_{11} = \sigma_{22} = \sigma_{12} = 0. \tag{6d}$$

Recall that, in a multiparameter strain gradient theory, the total strain energy stored in a continuum is composed of both the work done by Cauchy stress against strain and the one done by the double stress

with respect to strain gradient [Mindlin and Eshel 1968; Gao and Park 2007; Papargyri-Beskou et al. 2003]

$$U = \frac{1}{2}\int_{\Omega} (\tau_{ij}\,\varepsilon_{ij} + \mu_{ijk}\,\varepsilon_{ij,k})\,\mathrm{d}V. \tag{7}$$

Within the context of SSGET theory, the first variation of this strain energy function can be evaluated by the use of (1a), (1b), (1c), (2a)–(2f), (5a)–(5d), (6a)–(6d) and the divergence theorem

$$\begin{aligned}\delta U &= \int_{\Omega} \sigma_{ij}\,\delta\varepsilon_{ij}\,\mathrm{d}V + \int_{A} c\tau_{ij,k}\,n_k\,\delta\varepsilon_{ij}\,\mathrm{d}A \\ &= \int_{\Omega} (\sigma_{33}\,\delta\varepsilon_{33} + 2\sigma_{13}\,\delta\varepsilon_{13} + 2\sigma_{23}\,\delta\varepsilon_{23})\,\mathrm{d}V \\ &\quad + \int_{A} (c\tau_{33,k}\,n_k\,\delta\varepsilon_{33} + 2c\tau_{13,k}\,n_k\,\delta\varepsilon_{13} + 2c\tau_{23,k}\,n_k\,\delta\varepsilon_{23})\,\mathrm{d}A,\end{aligned} \tag{8}$$

where A is the area of both end surfaces of the rod. It should be noted that the boundary surface $\partial\Omega$ should include both the end and the lateral surfaces of the rod. However, in the surface integral, there is no contribution from the lateral surface because it is free of any traction, i.e.,

$$\tau_{11} = \tau_{22} = \tau_{12} = 0.$$

Such an assumption is the same as the one used for solving the torsion and bending deformation of prismatic bars only subjected to end loads in classical theory of elasticity. As a result, we only need to consider the surface integral on end cross-sections $S = L$ and $S = 0$. Moreover, the volume integral is formulated in terms of the total stresses (1a). From the first integrand of the volume integral, it there can be concluded that both the longitudinal and the transverse strain gradients of the bending stress/strain are included in the formulation. In addition, the second and the third integrands of the volume integral demonstrate that the shear strain gradient effects are also taken into account. The latter terms are not needed in higher-order elasticity theory of beams under pure bending.

In terms of (4a)–(4b) and noting $\boldsymbol{\theta} = \theta_i \boldsymbol{d}_i$, a relation bridging the rotational and the curvature vector can be derived:

$$\boldsymbol{\theta}' \cdot \boldsymbol{d}_i = \boldsymbol{\kappa} \cdot \boldsymbol{e}_i - \boldsymbol{\kappa}^0 \cdot \boldsymbol{d}_i \equiv \kappa_i - \kappa_i^0, \tag{9}$$

whose components are given by

$$\theta_1' - \kappa_3^0\theta_2 + \kappa_2^0\theta_3 = \kappa_1 - \kappa_1^0, \tag{10a}$$

$$\theta_2' + \kappa_3^0\theta_1 - \kappa_1^0\theta_3 = \kappa_2 - \kappa_2^0, \tag{10b}$$

$$\theta_3' - \kappa_2^0\theta_1 + \kappa_1^0\theta_2 = \kappa_3 - \kappa_3^0. \tag{10c}$$

For brevity, the development of (9) and (10a)–(10c) are detailed in the Appendix. In (10a)–(10c) and throughout the paper, the prime denotes the spatial derivative with respect to the centerline coordinate S, e.g., $\theta_1' = \partial\theta_1/\partial S$.

Substituting (2d)–(2f) and (10a)–(10c) into the first integral in (8) results in

$$\begin{aligned}\int_\Omega &(\sigma_{33}\delta\varepsilon_{33}+2\sigma_{13}\delta\varepsilon_{13}+2\sigma_{23}\delta\varepsilon_{23})\,\mathrm{d}V\\ &=-\int_0^L\big[\big(F_1'-\kappa_3^0F_2+\kappa_2^0F_3\big)\delta x_{01}+\big(F_2'+\kappa_3^0F_1-\kappa_1^0F_3\big)\delta x_{02}+\big(F_3'+\kappa_2^0F_1+\kappa_1^0F_2\big)\delta x_{03}\\ &\qquad+\big(M_1'-\kappa_3^0M_2+\kappa_2^0M_3-F_2+\kappa_2^0\Phi_1+\kappa_2^0\Phi_2\big)\delta\theta_1\\ &\qquad+\big(M_2'+\kappa_3^0M_1-\kappa_1^0M_3+F_1-\kappa_1^0\Phi_1-\kappa_1^0\Phi_2\big)\delta\theta_2\\ &\qquad+\big(M_3'-\kappa_2^0M_1+\kappa_1^0M_2+\Phi_1'+\Phi_2'\big)\delta\theta_3\big]\mathrm{d}s\\ &+\big[\big(F_1\delta x_{01}+F_2\delta x_{02}+F_3\delta x_{03}\big)\big]\big|_{s=0}^{s=L}+\left[M_1\delta\theta_1+M_2\delta\theta_2+(M_3+\Phi_1+\Phi_2)\,\delta\theta_3\right]\big|_{s=0}^{s=L},\end{aligned}\tag{11}$$

where L is the total length of the rod and

$$F_1\equiv\int_A\sigma_{31}\,\mathrm{d}A,\quad F_2\equiv\int_A\sigma_{32}\,\mathrm{d}A,\quad F_3\equiv\int_A\sigma_{33}\,\mathrm{d}A,\tag{12}$$

$$M_1\equiv\int_A Y\sigma_{33}\,\mathrm{d}A,\quad M_2\equiv\int_A-X\sigma_{33}\,\mathrm{d}A,\quad M_3\equiv\int_A(X\sigma_{32}-Y\sigma_{31})\,\mathrm{d}A,\tag{13}$$

$$\Phi_1\equiv\int_A\sigma_{13}\frac{\partial\varphi}{\partial X}\mathrm{d}A,\quad \Phi_2\equiv\int_A\sigma_{23}\frac{\partial\varphi}{\partial Y}\mathrm{d}A.\tag{14}$$

They stand for the resultant forces and moments, obtained by integrating the total stresses over the cross-sectional area. With the help of (2d)–(2f), (10a)–(10c) and the relations [Zhang and Gao 2019]

$$\frac{\partial x_{01}}{\partial S}-\kappa_3^0x_{02}+\kappa_2^0x_{03}=\theta_2,\quad \frac{\partial x_{02}}{\partial S}+\kappa_3^0x_{01}-\kappa_1^0x_{03}=-\theta_1,\quad \frac{\partial x_{03}}{\partial S}-\kappa_2^0x_{01}+\kappa_1^0x_{02}=\varepsilon,\tag{15}$$

the first variation of the second integral in (8) can also be determined:

$$\begin{aligned}&\left[\int_{\partial\Omega}(c\tau_{33,k}\delta\varepsilon_{33}+2c\tau_{13,k}\delta\varepsilon_{13}+2c\tau_{23,k}\delta\varepsilon_{23})\,\mathrm{d}A\right]_0^L\\ &\quad=\big[\big(\kappa_3^0M_2^G-\kappa_2^0M_3^G-\kappa_2^0\Phi_1^G-\kappa_2^0\Phi_2^G\big)\delta\theta_1+\big(-\kappa_3^0M_1^G+\kappa_1^0M_3^G+\kappa_1^0\Phi_1^G+\kappa_1^0\Phi_2^G\big)\delta\theta_2\\ &\qquad+\big(\kappa_2^0M_1^G-\kappa_1^0M_2^G\big)\delta\theta_3\big]\big|_{s=0}^{s=L}+\big[M_1^G\delta\theta_1'+M_2^G\delta\theta_2'+\big(M_3^G+\Phi_1^G+\Phi_2^G\big)\delta\theta_3'\big]\big|_{s=0}^{s=L},\end{aligned}\tag{16}$$

where

$$M_1^G\equiv\int_A Yc\tau_{33,k}\,\mathrm{d}A,\quad M_2^G\equiv\int_A-Xc\tau_{33,k}\,\mathrm{d}A,\quad M_3^G\equiv\int_A(Xc\tau_{32,k}-Yc\tau_{31,k})\,\mathrm{d}A,\tag{17}$$

$$\Phi_1^G\equiv\int_A c\tau_{13,k}\frac{\partial\varphi}{\partial X}\mathrm{d}A,\quad \Phi_2^G\equiv\int_A c\tau_{23,k}\frac{\partial\varphi}{\partial Y}\mathrm{d}A.\tag{18}$$

Within the context of the SSGET theory [Papargyri-Beskou et al. 2003], the virtual work done by the external forces acting on the rod can be written as

$$\delta W=\int_0^L(\boldsymbol{f}\cdot\delta\boldsymbol{x}_0+\boldsymbol{c}\cdot\delta\boldsymbol{\theta})\,\mathrm{d}S+(\overline{\boldsymbol{F}}\cdot\delta\boldsymbol{x}_0+\overline{\boldsymbol{M}}\cdot\delta\boldsymbol{\theta}+\overline{\boldsymbol{M}}^G\cdot\delta\boldsymbol{\theta}')\big|_0^L,\tag{19}$$

where $\boldsymbol{f}$ and $\boldsymbol{c}$ are the body force and body couple per unit length. The variables $\overline{\boldsymbol{F}}$, $\overline{\boldsymbol{M}}$ and $\overline{\boldsymbol{M}}^G$ are, respectively, the external force, bending moments and double bending moments applied at the ends of the rod.

According to the principle of minimum total potential energy [Reddy 2002], the first variation of the total potential energy vanishes under equilibrium state, i.e.,

$$\delta\Pi = \delta U - \delta W = 0. \tag{20}$$

With the help of the fundamental lemma of calculus of variations, the substitution of (8), (11), (16) and (19) into (20) yields the equilibrium equations

$$F_1' - \kappa_3^0 F_2 + \kappa_2^0 F_3 + f_1 = 0, \tag{21a}$$
$$F_2' + \kappa_3^0 F_1 - \kappa_1^0 F_3 + f_2 = 0, \tag{21b}$$
$$F_3' - \kappa_2^0 F_1 + \kappa_1^0 F_2 + f_3 = 0, \tag{21c}$$
$$M_1' - \kappa_3^0 M_2 + \kappa_2^0 M_3 - F_2 + \kappa_2^0 \Phi_1 + \kappa_2^0 \Phi_2 + c_1 = 0, \tag{21d}$$
$$M_2' + \kappa_3^0 M_1 - \kappa_1^0 M_3 + F_1 - \kappa_1^0 \Phi_1 - \kappa_1^0 \Phi_2 + c_2 = 0, \tag{21e}$$
$$M_3' - \kappa_2^0 M_1 + \kappa_1^0 M_2 + \Phi_1' + \Phi_2' + c_3 = 0, \tag{21f}$$

and the boundary conditions

$$F_1 = \overline{F}_1, \quad \text{or } x_{01} = \bar{x}_{01}, \tag{22a}$$
$$F_2 = \overline{F}_2, \quad \text{or } x_{02} = \bar{x}_{02}, \tag{22b}$$
$$F_3 = \overline{F}_3, \quad \text{or } x_{03} = \bar{x}_{03}, \tag{22c}$$
$$M_1 + \kappa_3^0 M_2^G - \kappa_2^0 M_3^G - \kappa_2^0 \Phi_1^G - \kappa_2^0 \Phi_2^G = \overline{M}_1, \quad \text{or } \theta_1 = \bar{\theta}_1, \tag{22d}$$
$$M_2 - \kappa_3^0 M_1^G + \kappa_1^0 M_3^G + \kappa_1^0 \Phi_1^G + \kappa_1^0 \Phi_2^G = \overline{M}_2, \quad \text{or } \theta_2 = \bar{\theta}_2, \tag{22e}$$
$$M_3 + \kappa_2^0 M_1^G - \kappa_1^0 M_2^G + \Phi_1 + \Phi_2 = \overline{M}_3, \quad \text{or } \theta_3 = \bar{\theta}_3, \tag{22f}$$
$$M_1^G = \overline{M}_1^G, \quad \text{or } \theta_1' = \bar{\theta}_1', \tag{22g}$$
$$M_2^G = \overline{M}_2^G, \quad \text{or } \theta_2' = \bar{\theta}_2', \tag{22h}$$
$$M_3^G + \Phi_1^G + \Phi_2^G = \overline{M}_3^G, \quad \text{or } \theta_3' = \bar{\theta}_3'. \tag{22i}$$

Note that, in (22a)–(22i), those variables with an overbar stand for prescribed values. It is noted that, by setting the initial curvatures to zero, the equilibrium equations (21a)–(21f) and the boundary conditions (22a)–(22i) reduce to the governing equations of straight rods. The equilibrium equations (21a)–(21f) and boundary conditions (22a)–(22i) can also be rewritten in a coordinate-invariant form, i.e.,

$$\boldsymbol{F}' + \boldsymbol{f} = \boldsymbol{0}, \quad \boldsymbol{M}' + \boldsymbol{\Phi}' + \boldsymbol{d}_3 \times \boldsymbol{F} + \boldsymbol{c} = \boldsymbol{0}, \tag{23}$$

and

$$\begin{aligned} &\boldsymbol{F} = F_1\boldsymbol{d}_1 + F_2\boldsymbol{d}_2 + F_3\boldsymbol{d}_3, \quad &&\boldsymbol{f} = f_1\boldsymbol{d}_1 + f_2\boldsymbol{d}_2 + f_3\boldsymbol{d}_3, \quad &&\boldsymbol{c}_f = c_2\boldsymbol{d}_1 - c_1\boldsymbol{d}_2, \\ &\boldsymbol{M} = M_1\boldsymbol{d}_1 + M_2\boldsymbol{d}_2 + M_3\boldsymbol{d}_3, \quad &&\boldsymbol{\Phi} = (\Phi_1 + \Phi_2)\,\boldsymbol{d}_3, \quad &&\boldsymbol{c} = c_1\boldsymbol{d}_1 + c_2\boldsymbol{d}_2 + 2c_3\boldsymbol{d}_3. \end{aligned} \tag{24}$$

It should be pointed out that this newly developed model, as an extension of the classical Kirchhoff rod theory based on the simplified strain gradient theory, has the same limitations as those of the classical Kirchhoff rod model.

For rods with a circular cross-section, the warping function vanishes, i.e., $\varphi(X, Y) = 0$. As a result, the equilibrium equations (21a)–(21f) simplify to

$$F_1' - \kappa_3 F_2 + \kappa_2 F_3 + f_1 = 0, \tag{25a}$$
$$F_2' + \kappa_3 F_1 - \kappa_1 F_3 + f_2 = 0, \tag{25b}$$
$$F_3' - \kappa_2 F_1 + \kappa_1 F_2 + f_3 = 0, \tag{25c}$$
$$M_1' - \kappa_3 M_2 + \kappa_2 M_3 - F_2 + c_1 = 0, \tag{25d}$$
$$M_2' + \kappa_3 M_1 - \kappa_1 M_3 + F_1 + c_2 = 0, \tag{25e}$$
$$M_3' - \kappa_2 M_1 + \kappa_1 M_2 + c_3 = 0. \tag{25f}$$

When the microstructure-dependent effects are absent, i.e., $c = 0$, equations (1c) and (1a) reduce to $\mu_{ijk} = 0$ and $\sigma_{ij} = \tau_{ij}$, respectively. Similarly, equations (12) and (13) represent the resultant forces and moments of Cauchy stress alone. Equations (25a)–(25f) therefore degenerate to the equilibrium conditions of a classical Kirchhoff rod [Dill 1992; Love 1944].

3. Applications

3.1. ***Equilibrium analysis of a microspring.*** Figure 2 shows a helical spring of radius r made of a uniform circular rod of radius r_{rod}. We consider that body forces and moments are absent, i.e., $f_1 = f_2 = f_3 = 0$ and $c_1 = c_2 = c_3 = 0$, and that the centerline of the undeformed rod is a straight line ($\kappa_i^0 = 0$). Based on the Euler angles in the deformed configuration $(\beta_1', \beta_2', \beta_3')$ [Coleman et al. 1993; Love 1944] the components of the curvature vector $\boldsymbol{\kappa}$ are given by

$$\kappa_1 = -\beta_1' \sin\beta_2 \cos\beta_3 + \beta_2' \sin\beta_3, \quad \kappa_2 = \beta_1' \sin\beta_2 \sin\beta_3 + \beta_2' \cos\beta_3, \quad \kappa_3 = \beta_3' + \beta_1' \cos\beta_2, \tag{26}$$

where β_1, β_2 and β_3 are three Euler angles associated with the base vectors $\boldsymbol{e}_i$ (Figure 2).

For the rod bent into a spring (Figure 2), one specific solution can be obtained by assuming $\beta_2 = \pi/2 - \alpha$ and β_1' and β_3' as constants [Love 1944]. For a given spring, the angle α between the centerline of the rod and the spring cross-section is also assumed a constant. With these assumptions, (26) simplifies to

$$\kappa_1 = -\beta_1' \cos\alpha \cos\beta_3, \tag{27a}$$
$$\kappa_2 = \beta_1' \cos\alpha \sin\beta_3, \tag{27b}$$
$$\kappa_3 = \beta_3' + \beta_1' \sin\alpha. \tag{27c}$$

From equations (6a)–(6d) and (13), the resultant moments acting on the rod cross-section can be expressed in terms of the three curvatures κ_1, κ_2 and κ_3:

$$M_1 = (1 - c\nabla^2) EI\kappa_1, \quad M_2 = (1 - c\nabla^2) EI\kappa_2, \quad M_3 = (1 - c\nabla^2) GJ\kappa_3, \tag{28}$$

where

$$I = \int_A X^2 \,\mathrm{d}A = \int_A Y^2 \,\mathrm{d}A, \quad J = \int_A (X^2 + Y^2) \,\mathrm{d}A, \tag{29}$$

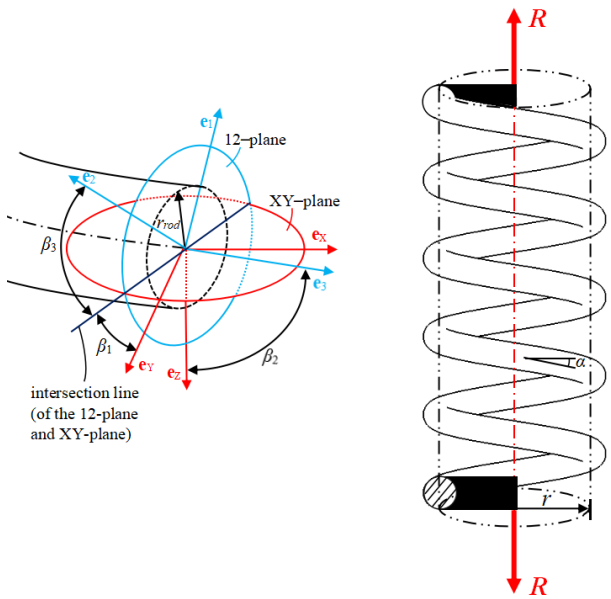

Figure 2. A microspring of radius r made by a uniform circular rod of radius r_{rod}.

are, respectively, the second moment of area and the polar moment of inertial of the circular cross-section. Substituting equations (28) into (25a)–(25f) yields

$$\frac{\partial}{\partial S}[(1-c\nabla^2)EI\kappa_1]-\kappa_3[(1-c\nabla^2)EI\kappa_2]+\kappa_2[(1-c\nabla^2)GJ\kappa_3]-F_2=0, \tag{30a}$$

$$\frac{\partial}{\partial S}[(1-c\nabla^2)EI\kappa_2]+\kappa_3[(1-c\nabla^2)EI\kappa_1]-\kappa_1[(1-c\nabla^2)GJ\kappa_3]+F_1=0, \tag{30b}$$

$$\frac{\partial}{\partial S}[(1-c\nabla^2)GJ\kappa_3]=0. \tag{30c}$$

From (27c), it is seen that the third component κ_3 of the curvature vector is a constant. Equation (30c) can therefore be automatically satisfied.

From static equilibrium, the resultant forces of stresses integrated over a rod cross-section must balance the restoring force R acting along the symmetry axis of the helix microspring [Love 1944]. Projections of the static equilibrium equation along the three local coordinate axes in the deformed configuration lead to

$$F_1=-R\cos\beta_3\cos\alpha, \tag{31a}$$

$$F_2=R\sin\beta_3\cos\alpha, \tag{31b}$$

$$F_3=R\sin\alpha. \tag{31c}$$

It can be readily shown that equations (27a)–(27c) and (31a)–(31c) satisfy the nonclassical equilibrium equations (25a)–(25f). Substituting (27a)–(27c) into (30a) and (30b) results in

$$F_1=-[(1+l^2)\,EI\beta_3'-(\beta_3'+\beta_1'\sin\alpha)(1+l^2)\,EI+GJ(1+l^2)(\beta_3'+\beta_1'\sin\alpha)]\beta_1'\cos\alpha\cos\beta_3, \tag{32a}$$

$$F_2=[(1+l^2)\,EI\beta_3'-(\beta_3'+\beta_1'\sin\alpha)(1+l^2)\,EI+(\beta_3'+\beta_1'\sin\alpha)(1+l^2)\,GJ]\beta_1'\cos\alpha\sin\beta_3, \tag{32b}$$

where $l^2 = c\beta_3'^2$, with c being the simplified strain gradient coefficient. Note that, for the present problem, α, β_1' and β_3' are all constants for the entire helical rod ($0 \le S \le L$). With $\kappa_i^0 = 0$, $\Phi_1 = \Phi_2 = 0$ and $\Phi_1^G = \Phi_2^G = 0$, these constants can ensure that all the resultants given by (12), (13) and (17) satisfy the boundary conditions (22a)–(22i). Equations (27a)–(27c) therefore represent an exact solution of the helical rod problem based on the developed nonclassical Kirchhoff rod model.

Comparing (32a) and (32b) with (31a) and (31b), it then follows that

$$R = [(\beta_3' + \beta_1' \sin\alpha) GJ - \beta_1' \sin\alpha EI](1 + l^2)\beta_1'. \tag{33}$$

It is worth noting that the third component κ_3 of the curvature vector is composed of two parts as in (27c): the internal twist β_3' and the tortuosity $1/\Sigma = \beta_1' \sin\alpha$. In terms of the radius r of the microspring, the measure of tortuosity is found to be [Love 1944]

$$\frac{1}{\Sigma} = \sin\alpha \frac{\cos\alpha}{r} = \beta_1' \sin\alpha. \tag{34}$$

The restoring force R can then be calculated as

$$R = \left[\beta_3' GJ + (GJ - EI)\frac{\sin\alpha\cos\alpha}{r}\right](1 + l^2)\frac{\cos\alpha}{r}. \tag{35}$$

When the microstructure-dependent effects are absent by setting $c = 0$, the material length squared constant also becomes zero ($l^2 = 0$). As a result, equation (35) reduces to

$$R_C = GJ\left(\beta_3' + \frac{\sin\alpha\cos\alpha}{r}\right)\frac{\cos\alpha}{r} - EI\frac{\sin\alpha\cos^2\alpha}{r^2}. \tag{36}$$

Equation (36) is identical to the classical restoring force exerted by a Kirchhoff rod bent into a helical spring [Love 1944]. Equations (35) and (36) clearly show that the incorporation of the microstructural effects will always lead to the increase of the restoring force R.

Figure 3 shows the variation of the restoring force R predicted by the proposed SSGET rod model

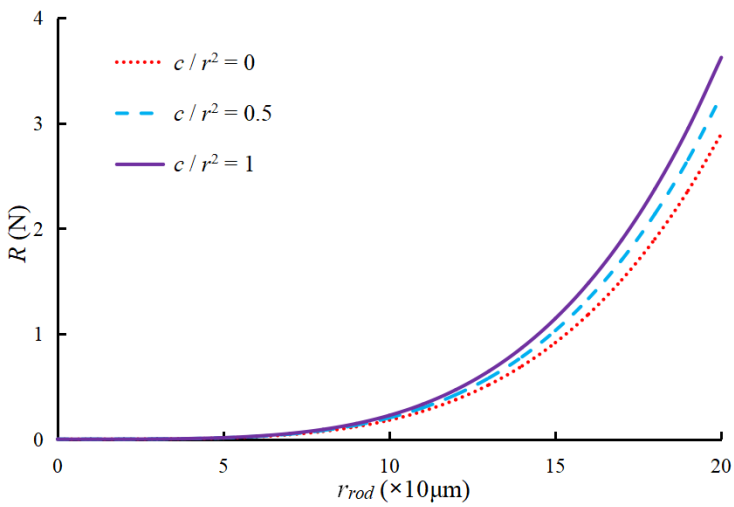

Figure 3. Variation of the microspring restoring force R as a function of the rod radius (r_{rod}) and the dimensionless strength of the microstructural effects (c/r^2).

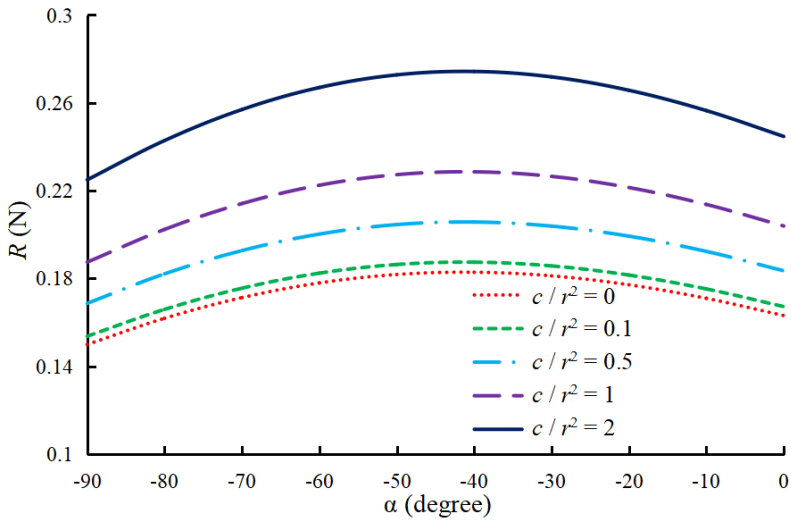

Figure 4. Variation of the microspring restoring force R as a function of the angle α and the dimensionless strength of the microstructural effects (c/r^2).

as a function of the rod radius (r_{rod}) and the strength of microstructural effects (c/r^2). For comparison purpose, the classical solution $(c/r^2 = 0)$ is also plotted in the figure. The isotropic material properties used in the calculations are assumed to be $E = 135\,\text{GPa}$ and $v = 0.3$ [Gao and Park 2007]. The constant angle α is taken as $-30°$ and the dimensionless constant β_3' is set to be 100. The radius of the microspring r is taken to be 5 mm.

From Figure 3, it is clearly seen that the restoring force R predicted by both the proposed SSGET rod model and its classical counterpart increases with the rod radius. This behavior follows the general trend and is physically natural. It is interesting to note that the restoring force R predicted by the proposed SSGET rod model is always larger than that of the classical solution. This means that the classical solution underestimates the restoring force of a microspring. The incorporation of the microstructure-dependent effects helps stiffen the microspring. In addition, the difference between the predicted nonclassical restoring force and its classical counterpart increases with the simplified strain gradient coefficient.

To further illustrate the microstructure-dependent effects with the proposed SSGET rod model, the variation of the spring restoring force R as a function of the angle α is shown in Figure 4. In this case, the rod radius is fixed as a constant, i.e., $r_{\text{rod}} = 100\,\mu\text{m}$. For comparison purpose, the restoring force R calculated from the classical model is also presented in the figure. Other material properties and parameters assume the same values as those employed for Figure 3. The restoring force R is calculated for all possible values of the angle α, i.e., $(-\pi/2, 0)$. It is seen that the restoring force varies parabolically with the angle α. For all simplified strain gradient coefficients, the maximum restoring force occurs approximately at $\alpha = -40°$. As expected, the restoring force also increases with the simplified strain gradient coefficient c/r^2.

3.2. ***Buckling analysis of a microcolumn.*** Let us consider a simply supported microcolumn with uniform circular cross-section. The centerline of the undeformed column is a straight line with zero initial curvatures $\kappa_i^0 = 0$, as shown in Figure 5. The microcolumn is pinned at the base $(S = 0)$ and subjected to a

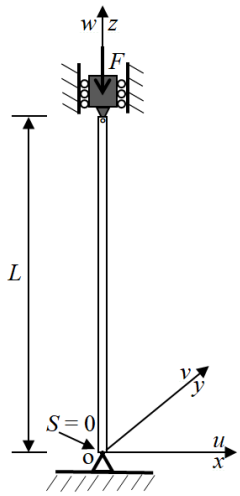

Figure 5. A simply supported microcolumn subjected to an axial compressive force.

compressive axial force F at another pinned end ($S = L$). For small compressive forces, the microcolumn is simply under axial contraction. However, with increased F, buckling occurs in the form of a sudden transverse deflection.

Let u and v be the transverse displacements along the x- and y-directions. The rotation around the centerline of the microcolumn is denoted by γ. Note that u, v and γ are all measured with reference to the unbuckled state, i.e., $u = x_{01}$, $v = x_{02}$ and $\gamma = \theta_3$. Under this condition, the components of the curvature vector $\boldsymbol{\kappa}$ becomes [Love 1944]

$$\kappa_1 = -\frac{\partial^2 v}{\partial S^2}, \quad \kappa_2 = \frac{\partial^2 u}{\partial S^2}, \quad \kappa_3 = \frac{\partial \gamma}{\partial S}. \tag{37}$$

From (6a)–(6d), (13) and (37), the resultant moments of the stresses can be expressed in terms of u, v and β as

$$M_1 = EI\left(-\frac{\partial^2 v}{\partial S^2} + c\frac{\partial^4 v}{\partial S^4}\right), \quad M_2 = EI\left(\frac{\partial^2 u}{\partial S^2} - c\frac{\partial^4 u}{\partial S^4}\right), \quad M_3 = GJ\left(\frac{\partial \gamma}{\partial S} - c\frac{\partial^3 \gamma}{\partial S^3}\right). \tag{38}$$

In the absence of body forces and body moments, i.e., $f_1 = f_2 = f_3 = 0$ and $c_1 = c_2 = c_3 = 0$, substituting (37) and (38) back into (25d)–(25f) yields

$$F_1 = -EI\left(\frac{\partial^3 u}{\partial S^3} - c\frac{\partial^5 u}{\partial S^5}\right) - EI\left(-\frac{\partial^2 v}{\partial S^2}\frac{\partial \gamma}{\partial S} + c\frac{\partial^4 v}{\partial S^4}\frac{\partial \gamma}{\partial S}\right) - GJ\left(\frac{\partial \gamma}{\partial S}\frac{\partial^2 v}{\partial S^2} - c\frac{\partial^3 \gamma}{\partial S^3}\frac{\partial^2 v}{\partial S^2}\right), \tag{39a}$$

$$F_2 = EI\left(-\frac{\partial^3 v}{\partial S^3} + c\frac{\partial^5 v}{\partial S^5}\right) - EI\left(\frac{\partial^2 u}{\partial S^2}\frac{\partial \gamma}{\partial S} - c\frac{\partial^4 u}{\partial S^4}\frac{\partial \gamma}{\partial S}\right) + GJ\left(\frac{\partial \gamma}{\partial S}\frac{\partial^2 u}{\partial S^2} - c\frac{\partial^3 \gamma}{\partial S^3}\frac{\partial^2 u}{\partial S^2}\right), \tag{39b}$$

$$GJ\left(\frac{\partial^2 \gamma}{\partial S^2} - c\frac{\partial^4 \gamma}{\partial S^4}\right) - \frac{\partial^2 u}{\partial S^2}EI\left(c\frac{\partial^4 v}{\partial S^4}\right) + \frac{\partial^2 v}{\partial S^2}EI\left(c\frac{\partial^4 u}{\partial S^4}\right) = 0. \tag{39c}$$

With the help of (15), (22a)–(22i), (38) and in view of the zero initial curvatures $\kappa_i^0 = 0$, the boundary conditions for the simply supported microcolumn with a circular cross section can be identified, i.e.,

$$u|_{S=0} = 0, \qquad \left.\frac{\partial^2 u}{\partial S^2}\right|_{S=0} = 0, \qquad \left.\frac{\partial^4 u}{\partial S^4}\right|_{S=0} = 0, \tag{40a}$$

$$v|_{S=0} = 0, \qquad \left.\frac{\partial^2 v}{\partial S^2}\right|_{S=0} = 0, \qquad \left.\frac{\partial^4 v}{\partial S^4}\right|_{S=0} = 0, \tag{40b}$$

$$F_3|_{S=0} = -F, \tag{40c}$$

$$\left.\frac{\partial \gamma}{\partial S}\right|_{S=0} = 0, \qquad \left.\left(\frac{\partial \gamma}{\partial S} - c\frac{\partial^3 \gamma}{\partial S^3}\right)\right|_{S=0} = 0, \tag{40d}$$

at the lower end ($S = 0$), and

$$u|_{S=L} = 0, \qquad \left.\frac{\partial^2 u}{\partial S^2}\right|_{S=L} = 0, \qquad \left.\frac{\partial^4 u}{\partial S^4}\right|_{S=L} = 0, \tag{41a}$$

$$v|_{S=L} = 0, \qquad \left.\frac{\partial^2 v}{\partial S^2}\right|_{S=L} = 0, \qquad \left.\frac{\partial^4 v}{\partial S^4}\right|_{S=L} = 0, \tag{41b}$$

$$F_3|_{S=L} = -F, \tag{41c}$$

$$\left.\frac{\partial \gamma}{\partial S}\right|_{S=L} = 0, \qquad \left.\left(\frac{\partial \gamma}{\partial S} - c\frac{\partial^3 \gamma}{\partial S^3}\right)\right|_{S=L} = 0, \tag{41d}$$

at the upper end ($S = L$).

It is noted that the transverse displacements u and v satisfy the same type of governing equations, due to the axial symmetry property of the circular microcolumn. Given the boundary conditions (40d) and (41d), the solution to (39c) is found to be

$$\gamma = 0, \tag{42}$$

for the entire microcolumn. From this and the equation $\kappa_3 = \dfrac{\partial \gamma}{\partial S}$ in (37), it then follows that

$$\kappa_3 = 0. \tag{43}$$

Substituting (42) into (39a) and (39b) yields

$$F_1 = -EI\left(\frac{\partial^3 u}{\partial S^3} - c\frac{\partial^5 u}{\partial S^5}\right), \qquad F_2 = EI\left(-\frac{\partial^3 v}{\partial S^3} + c\frac{\partial^5 v}{\partial S^5}\right). \tag{44}$$

With the help of (40c) and (41c), equation (25c) leads to

$$F_3 = -F. \tag{45}$$

Plugging (45) and (44) into (25a) and (25b) results in

$$EI\left(\frac{\partial^4 u}{\partial S^4} - c\frac{\partial^6 u}{\partial S^6}\right) + F\frac{\partial^2 u}{\partial S^2} = 0, \qquad EI\left(\frac{\partial^4 v}{\partial S^4} - c\frac{\partial^6 v}{\partial S^6}\right) + F\frac{\partial^2 v}{\partial S^2} = 0. \tag{46}$$

From (46), it can be clearly seen that the transverse displacements u and v satisfy the same sixth-order ordinary differential equation, as expected. Equations (46) can then be combined to a single equation

$$\frac{\partial^6 u}{\partial S^6} - a_1 \frac{\partial^4 u}{\partial S^4} - a_2 \frac{\partial^2 u}{\partial S^2} = 0, \tag{47}$$

where the constant coefficients are defined by

$$a_1 = \frac{1}{c}, \quad a_2 = \frac{F}{EIc}. \tag{48}$$

The characteristic equation of (47) can be easily found:

$$\lambda^6 - a_1 \lambda^4 - a_2 \lambda^2 = 0. \tag{49}$$

Its six roots are given by

$$\lambda_{1,2,3,4} = \pm \sqrt{\frac{a_1 \pm \sqrt{a_1^2 + 4a_2}}{2}}, \quad \lambda_{5,6} = 0. \tag{50}$$

At this point, the general solution to the transverse deflections $u(S)$ and $v(S)$ becomes straightforward:

$$u(S) = C_1 \cosh(\eta_1 S) + C_2 \sinh(\eta_1 S) + C_3 \cos(\eta_2 S) + C_4 \sin(\eta_2 S) + C_5 S + C_6, \tag{51}$$

where

$$\eta_1^2 = \frac{\sqrt{a_1^2 + 4a_2} + a_1}{2}, \quad \eta_2^2 = \frac{\sqrt{a_1^2 + 4a_2} - a_1}{2}. \tag{52}$$

Substituting (51) back into (40a) and (41a) leads to

$$C_1 + C_3 + C_6 = 0, \tag{53a}$$

$$\eta_1^2 C_1 - \eta_2^2 C_3 = 0, \tag{53b}$$

$$\eta_1^4 C_1 - \eta_2^4 C_3 = 0, \tag{53c}$$

$$\cosh(\eta_1 L) C_1 + \sinh(\eta_1 L) C_2 + \cos(\eta_2 L) C_3 + \sin(\eta_2 L) C_4 + L C_5 + C_6 = 0, \tag{53d}$$

$$\eta_1^2 \cosh(\eta_1 L) C_1 + \eta_1^2 \sinh(\eta_1 L) C_2 - \eta_2^2 \cos(\eta_2 L) C_3 - \eta_2^2 \sin(\eta_2 L) C_4 = 0, \tag{53e}$$

$$\eta_1^4 \cosh(\eta_1 L) C_1 + \eta_1^4 \sinh(\eta_1 L) C_2 + \eta_2^4 \cos(\eta_2 L) C_3 + \eta_2^4 \sin(\eta_2 L) C_4 = 0. \tag{53f}$$

Nontrivial solutions of (53a)–(53f) require that

$$\begin{vmatrix} 1 & 0 & 1 & 0 & 0 & 1 \\ \eta_1^2 & 0 & -\eta_2^2 & 0 & 0 & 0 \\ \eta_1^4 & 0 & \eta_2^4 & 0 & 0 & 0 \\ \cosh(\eta_1 L) & \sinh(\eta_1 L) & \cos(\eta_2 L) & \sin(\eta_2 L) & L & 1 \\ \eta_1^2 \cosh(\eta_1 L) & \eta_1^2 \sinh(\eta_1 L) & -\eta_2^2 \cos(\eta_2 L) & -\eta_2^2 \sin(\eta_2 L) & 0 & 0 \\ \eta_1^4 \cosh(\eta_1 L) & \eta_1^4 \sinh(\eta_1 L) & \eta_2^4 \cos(\eta_2 L) & \eta_2^4 \sin(\eta_2 L) & 0 & 0 \end{vmatrix} = L \eta_1^4 \eta_2^4 (\eta_1^2 + \eta_2^2)^2 \sinh(\eta_1 L) \sin(\eta_2 L) = 0. \tag{54}$$

The smallest root of (54) is

$$\eta_2 L = \pi. \tag{55}$$

From (48), (52) and (55), the critical value for the compressive force F can further be determined as

$$F_{\mathrm{cr}} = \frac{EI\pi^2}{L^2}\left(1 + c\frac{\pi^2}{L^2}\right). \tag{56}$$

Equation (56) shows that the critical buckling load F_{cr} is clearly dependent on the simplified strain gradient coefficient. This equation is also the same as that of a simply supported Bernoulli–Euler beam based on the SSGET model [Papargyri-Beskou et al. 2003]. In the absence of microstructure-dependent effects, i.e., $c = 0$, equations (46) can be further reduced to

$$EI\frac{\partial^4 u}{\partial S^4} + F\frac{\partial^2 u}{\partial S^2} = 0, \quad EI\frac{\partial^4 v}{\partial S^4} + F\frac{\partial^2 v}{\partial S^2} = 0. \tag{57}$$

For such a degenerated case, closed-form analytical solutions to both transverse deflections are obvious:

$$u(S) = D_1\cos\left(\sqrt{\frac{F}{EI}}S\right) + D_2\sin\left(\sqrt{\frac{E}{EI}}S\right) + D_3S + D_4. \tag{58}$$

Substituting (58) into (40a) and (41a) results in

$$D_1 = D_3 = D_4 = 0, \quad D_2\sin\left(\sqrt{\frac{F}{EI}}L\right) = 0. \tag{59}$$

The smallest root of this last equation is found to be

$$\sqrt{\frac{F_{\mathrm{cr}}^C}{EI}}L = \pi. \tag{60}$$

The critical buckling load F_{cr}^C can therefore be expressed as

$$F_{\mathrm{cr}}^C = \frac{EI\pi^2}{L^2}. \tag{61}$$

It is noted that (61) can also be reduced from (56) by setting the strain gradient parameter c to zero. Normalizing (56) with respect to (61) leads to

$$\frac{F_{\mathrm{cr}}}{F_{\mathrm{cr}}^C} = 1 + c\frac{\pi^2}{L^2}. \tag{62}$$

From this ratio, it is apparent that the critical buckling force increases with increased strain gradient coefficient c and decreased column length L. For positive c, this ratio is always greater than unity, indicating the stiffening nature of the strain gradient effects. Figure 6 shows the variation of this ratio as a function of the microcolumn length. The simplified strain gradient parameter is fixed as $c = 100\,\mu\mathrm{m}^2$. It can be observed from Figure 6 that, for short microcolumns, the critical buckling force predicted by the proposed model is significantly larger than its classical counterpart. Only for long columns, this ratio converges to unity.

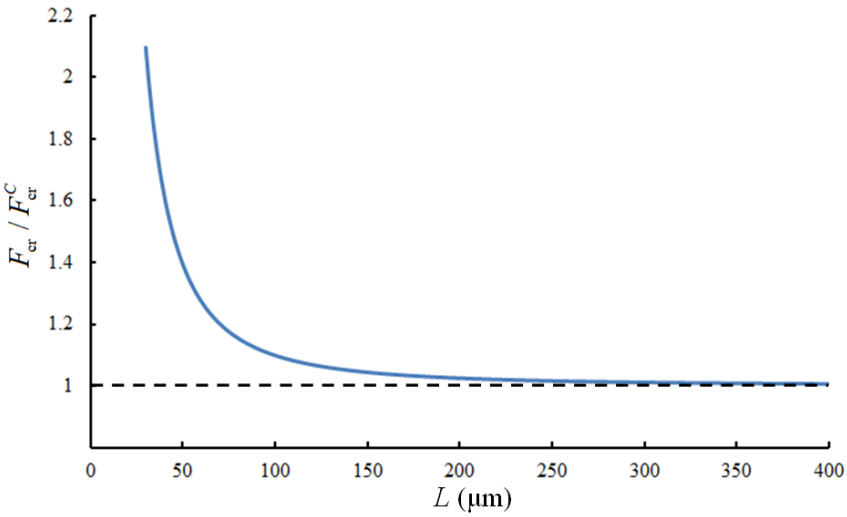

Figure 6. Variation of the dimensionless critical force resulting from the simplified strain gradient model as a function of column length.

Within the context of modified couple stress theory [Zhang and Gao 2019], the critical buckling load for a simply supported microcolumn as shown in Figure 5 can be expressed by

$$F_{\mathrm{cr}}^{M} = \frac{EI\pi^2}{L^2}\left[1 + \frac{(1+2v)^2 l_m^2}{2(1+v)r_{\mathrm{rod}}^2}\right], \tag{63}$$

where l_m represents a material length scale parameter measuring the couple stress effect [Mindlin 1963].

For comparison purpose, let us now consider the ratio between (63) and its classical counterpart

$$\frac{F_{\mathrm{cr}}^{M}}{F_{\mathrm{cr}}^{C}} = 1 + \frac{(1+2v)^2 l_m^2}{2(1+v)r_{\mathrm{rod}}^2}, \tag{64}$$

From the above equation, it is clear that the critical buckling load due to the modified couple stress theory is always greater than its classical value for any nonzero l_m. This observation again demonstrates stiffening effects of the modified couple stress model, as illustrated in Figure 7. The two parameters involved in (64) are fixed as $v = 0$ and $l = 10\,\mu$m.

Based on above discussions, it is clear that both the simplified strain gradient model and the modified couple stress theory are helpful to elevate the critical buckling force of a simply supported microcolumn. The effects of both theories can be very significant for small sized columns. However, some differences do exist. While the SSGET critical force is directly dependent on the column length L, the prediction resulting from the modified couple stress theory is up to the column radius r_{rod}. Depending on the specific higher-order theory that is incorporated in the buckling analysis of a microcolumn, one geometric parameter may become more important than another.

The analysis conducted in the present subsection is valid for a simply supported microcolumn. For other boundary conditions, the corresponding critical buckling forces can be derived by following the same procedure.

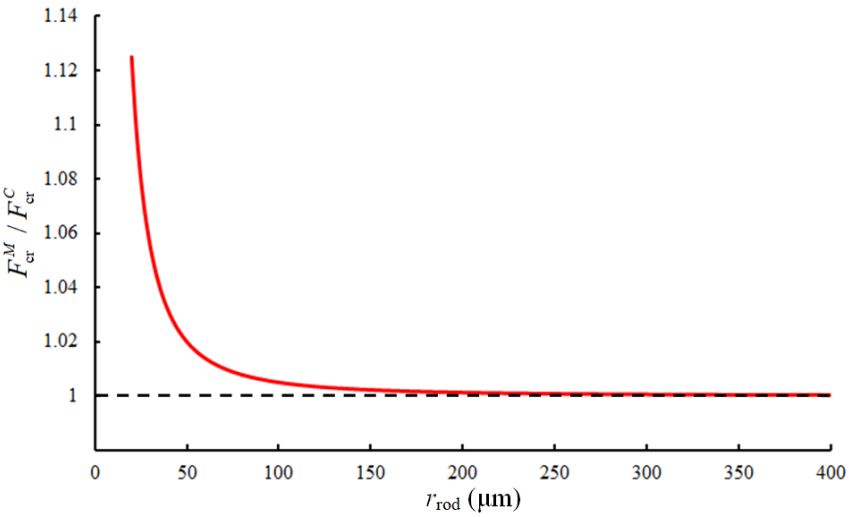

Figure 7. Variation of the dimensionless critical force resulting from the modified couple stress theory as a function of column radius.

4. Conclusions

Within the context of the simplified strain gradient elasticity theory, a nonclassical Kirchhoff rod model has been presented. A single intrinsic material length squared parameter was introduced in the model in order to account for the effects of microstructures. The longitudinal, transverse and shear strain gradient effects were all taken into account through a standard variational approach. To illustrate the proposed nonclassical rod model, two boundary value problems dealing with the static equilibrium of a microspring and the buckling behavior of a microcolumn were analytically solved. Some important features are concluded as follows.

(1) Both the equilibrium equations and the complete set of boundary conditions are analytically determined for this new nonclassical rod model which incorporates the microstructure effect.

(2) For the microspring that was deformed from an originally straight uniform rod, the restoring force has been underestimated by the classical Kirchhoff rod theory. In the presence of microstructural effects, the restoring force is found to monotonically increase with both the rod radius and the strength of the simplified strain gradient coefficient.

(3) For a simply supported microcolumn, its critical buckling force was analytically solved by directly applying the governing equations and boundary conditions of the presented model. Both the analytical solution and numerical results show that the critical buckling load resulting from the nonclassical rod model is appreciably larger than its classical counterpart. The stiffening size effects are also found to be consistent with those due to the modified couple stress theory.

Despite its advantages, it is worth noting that this newly developed model possesses the same limitations as those of the classical Kirchhoff rod model.

Appendix

Here, the relation between the small rotation vector and curvatures given in (9) is derived. The orthonormal base vectors $\boldsymbol{d}_i(S)$ and $\boldsymbol{e}_i(S)$ are related by [Zhang and Gao 2019]

$$\boldsymbol{e}_i(S) = \boldsymbol{Q}(S)\,\boldsymbol{d}_i(S), \tag{A.1}$$

where $\boldsymbol{Q} = \boldsymbol{e}_i \otimes \boldsymbol{d}_i$ is a rotation tensor possessing the properties $\boldsymbol{Q}^{-1} = \boldsymbol{Q}^T$ and $\det \boldsymbol{Q} = 1$. From Figure 1, the rotation tensor $\boldsymbol{Q}(S)$ can be approximated by [Bîrsan and Altenbach 2011]

$$\boldsymbol{Q}(S) = \boldsymbol{I} + \boldsymbol{\Theta}(S), \tag{A.2}$$

where $\boldsymbol{I}$ is the second-order identity tensor, and $\boldsymbol{\Theta}(S)$ is a skew tensor that is related to its axial vector $\boldsymbol{\theta}(S)$ (a small rotation) through

$$\boldsymbol{\Theta}\boldsymbol{d}_i = \boldsymbol{\theta} \times \boldsymbol{d}_i. \tag{A.3}$$

From (4a) and (A.3), it follows that

$$\boldsymbol{\theta}' \cdot \boldsymbol{d}_i = \tfrac{1}{2}(\boldsymbol{d}_i \times \boldsymbol{\Theta}\boldsymbol{d}_i)' \cdot \boldsymbol{d}_i = \tfrac{1}{2}\{-[(\boldsymbol{\kappa}^0 \times \boldsymbol{d}_i)\cdot\boldsymbol{\theta}]\boldsymbol{d}_i + \boldsymbol{d}_i \times (\boldsymbol{\Theta}\boldsymbol{d}_i)'\} \cdot \boldsymbol{d}_i, \tag{A.4}$$

The combination of (4b), (A.1), (A.2) and (A.3) yields

$$\begin{aligned}\boldsymbol{\kappa}\cdot\boldsymbol{e}_i &= \tfrac{1}{2}(\boldsymbol{e}_i \times \boldsymbol{e}_i')\cdot\boldsymbol{e}_i = \tfrac{1}{2}[\,\boldsymbol{Q}\boldsymbol{d}_i \times (\boldsymbol{Q}\boldsymbol{d}_i)']\cdot\boldsymbol{Q}\boldsymbol{d}_i \\ &= \tfrac{1}{2}[\boldsymbol{d}_i \times \boldsymbol{d}_i' + \boldsymbol{d}_i \times (\boldsymbol{\Theta}\boldsymbol{d}_i)' + (\boldsymbol{\Theta}\boldsymbol{d}_i)\times\boldsymbol{d}_i' + (\boldsymbol{\theta}\cdot\boldsymbol{d}_i)\boldsymbol{d}_i' - (\boldsymbol{\theta}\cdot\boldsymbol{d}_i')\cdot\boldsymbol{d}_i]\cdot\boldsymbol{d}_i + O(o^2).\end{aligned} \tag{A.5}$$

From (4a) one has

$$\boldsymbol{\kappa}^0 \cdot \boldsymbol{d}_i = \tfrac{1}{2}(\boldsymbol{d}_i \times \boldsymbol{d}_i')\cdot\boldsymbol{d}_i. \tag{A.6}$$

It follows from (A.5) and (A.6) that

$$\begin{aligned}\boldsymbol{\kappa}\cdot\boldsymbol{e}_i - \boldsymbol{\kappa}^0\cdot\boldsymbol{d}_i &= \tfrac{1}{2}[\boldsymbol{d}_i \times (\boldsymbol{\Theta}\boldsymbol{d}_i)' + (\boldsymbol{\Theta}\boldsymbol{d}_i)\times\boldsymbol{d}_i' + (\boldsymbol{\theta}\cdot\boldsymbol{d}_i)\boldsymbol{d}_i' - (\boldsymbol{\theta}\cdot\boldsymbol{d}_i')\cdot\boldsymbol{d}_i]\cdot\boldsymbol{d}_i \\ &= \tfrac{1}{2}[\boldsymbol{d}_i \times (\boldsymbol{\Theta}\boldsymbol{d}_i)' + (\boldsymbol{\theta}\cdot\boldsymbol{d}_i)(\boldsymbol{\kappa}^0\times\boldsymbol{d}_i)]\cdot\boldsymbol{d}_i.\end{aligned} \tag{A.7}$$

The further use of (A.4) and (A.7) leads to (9)

$$\boldsymbol{\theta}'\cdot\boldsymbol{d}_i - (\boldsymbol{\kappa}\cdot\boldsymbol{e}_i - \boldsymbol{\kappa}^0\cdot\boldsymbol{d}_i) = \tfrac{1}{2}\{-[(\boldsymbol{\kappa}^0\times\boldsymbol{d}_i)\cdot\boldsymbol{\theta}]\boldsymbol{d}_i - (\boldsymbol{\theta}\cdot\boldsymbol{d}_i)(\boldsymbol{\kappa}^0\times\boldsymbol{d}_i)\}\cdot\boldsymbol{d}_i = 0. \tag{A.8}$$

Acknowledgements

We gratefully acknowledge the support from National Key R&D Program of China (grant number 2018YFD1100401) and National Natural Science Foundation of China (grant numbers 11872149 and 11772091). The authors would also like to thank Professor Adair R. Aguiar and three anonymous reviewers for their valuable discussions and comments on the earlier versions of this paper.

References

[Altan and Aifantis 1997] B. S. Altan and E. C. Aifantis, "On some aspects in the special theory of gradient elasticity", *J. Mech. Behav. Mater.* **8**:3 (1997), 231–282.

[Ansari et al. 2012] R. Ansari, R. Gholami, and M. A. Darabi, "A nonlinear Timoshenko beam formulation based on strain gradient theory", *J. Mech. Mater. Struct.* **7**:2 (2012), 195–211.

[Ansari et al. 2014] R. Ansari, A. Norouzzadeh, R. Gholami, M. F. Shojaei, and M. Hosseinzadeh, "Size-dependent nonlinear vibration and instability of embedded fluid-conveying SWBNNTs in thermal environment", *Physica E* **61** (2014), 148–157.

[Ansari et al. 2015] R. Ansari, R. Gholami, A. Norouzzadeh, and S. Sahmani, "Size-dependent vibration and instability of fluid-conveying functionally graded microshells based on the modified couple stress theory", *Microfluid. Nanofluid.* **19** (2015), 509–522.

[Bǐrsan and Altenbach 2011] M. Bǐrsan and H. Altenbach, "On the theory of porous elastic rods", *Int. J. Solids Struct.* **48**:6 (2011), 910–924.

[Burgner-Kahrs et al. 2015] J. Burgner-Kahrs, D. C. Rucker, and H. Choset, "Continuum robots for medical applications: a survey", *IEEE Trans. Robot.* **31**:6 (2015), 1261–1280.

[Chen et al. 2019] W. Chen, L. Wang, and H.-L. Dai, "Nonlinear free vibration of nanobeams based on nonlocal strain gradient theory with the consideration of thickness-dependent size effect", *J. Mech. Mater. Struct.* **14**:1 (2019), 119–137.

[Coleman et al. 1993] B. D. Coleman, E. H. Dill, M. Lembo, Z. Lu, and I. Tobias, "On the dynamics of rods in the theory of Kirchhoff and Clebsch", *Arch. Ration. Mech. Anal.* **121** (1993), 339–359.

[Dill 1992] E. H. Dill, "Kirchhoff's theory of rods", *Arch. Hist. Exact Sci.* **44**:1 (1992), 1–23.

[Eringen 1983] A. C. Eringen, "On differential equations of nonlocal elasticity and solutions of screw dislocation and surface waves", *J. Appl. Phys.* **54**:9 (1983), 4703–4710.

[Eslami-Mossallam and Ejtehadi 2009] B. Eslami-Mossallam and M. R. Ejtehadi, "Asymmetric elastic rod model for DNA", *Phys. Rev. E* **80**:1 (2009), 011919.

[Gao and Ma 2009] X.-L. Gao and H. M. Ma, "Green's function and Eshelby's tensor based on a simplified strain gradient elasticity theory", *Acta Mech.* **207** (2009), 163–181.

[Gao and Ma 2010] X.-L. Gao and H. M. Ma, "Strain gradient solution for Eshelby's ellipsoidal inclusion problem", *Proc. R. Soc. Lond. A* **466**:2120 (2010), 2425–2446.

[Gao and Park 2007] X.-L. Gao and S. K. Park, "Variational formulation of a simplified strain gradient elasticity theory and its application to a pressurized thick-walled cylinder problem", *Int. J. Solids Struct.* **44**:22-23 (2007), 7486–7499.

[Gao et al. 2009] X.-L. Gao, S. K. Park, and H. M. Ma, "Analytical solution for a pressurized thick-walled spherical shell based on a simplified strain gradient elasticity theory", *Math. Mech. Solids* **14**:8 (2009), 747–758.

[Georgiadis et al. 2004] H. G. Georgiadis, I. Vardoulakis, and E. G. Velgaki, "Dispersive Rayleigh-wave propagation in microstructured solids characterized by dipolar gradient elasticity", *J. Elasticity* **74** (2004), 17–45.

[Gourgiotis and Georgiadis 2009] P. A. Gourgiotis and H. G. Georgiadis, "Plane-strain crack problems in microstructured solids governed by dipolar gradient elasticity", *J. Mech. Phys. Solids* **57**:11 (2009), 1898–1920.

[Gurtin and Murdoch 1975] M. E. Gurtin and A. I. Murdoch, "A continuum theory of elastic material surfaces", *Arch. Ration. Mech. Anal.* **57** (1975), 291–323.

[Gurtin and Murdoch 1978] M. E. Gurtin and A. I. Murdoch, "Surface stress in solids", *Int. J. Solids Struct.* **14**:6 (1978), 431–440.

[Lakes 2018] R. S. Lakes, "Stability of Cosserat solids: size effects, ellipticity and waves", *J. Mech. Mater. Struct.* **13**:1 (2018), 83–91.

[Lam et al. 2003] D. C. C. Lam, F. Yang, A. C. M. Chong, J. Wang, and P. Tong, "Experiments and theory in strain gradient elasticity", *J. Mech. Phys. Solids* **51**:8 (2003), 1477–1508.

[Lazopoulos 2003] K. A. Lazopoulos, "Post-buckling problems for long elastic beams", *Acta Mech.* **164** (2003), 189–198.

[Lazopoulos 2004] K. A. Lazopoulos, "On the gradient strain elasticity theory of plates", *Eur. J. Mech. A Solids* **23**:5 (2004), 843–852.

[Lazopoulos and Lazopoulos 2010] K. A. Lazopoulos and A. K. Lazopoulos, "Bending and buckling of thin strain gradient elastic beams", *Eur. J. Mech. A Solids* **29**:5 (2010), 837–843.

[Lembo 2016] M. Lembo, "On nonlinear deformations of nonlocal elastic rods", *Int. J. Solids Struct.* **90** (2016), 215–227.

[Liangruksa et al. 2017] M. Liangruksa, T. Laomettachit, and S. Wongwises, "Theoretical study of DNA's deformation and instability subjected to mechanical stress", *Int. J. Mech. Sci.* **130** (2017), 324–330.

[Liu and Wang 2009] D. S. Liu and C. H.-T. Wang, "Variational principle for a special Cosserat rod", *Appl. Math. Mech.* **30** (2009), 1169–1176.

[Love 1944] A. E. H. Love, *A treatise on the mathematical theory of elasticity*, Dover Publications, New York, 1944.

[Lurie and Solyaev 2018] S. Lurie and Y. Solyaev, "Revisiting bending theories of elastic gradient beams", *Int. J. Eng. Sci.* **126** (2018), 1–21.

[McIlroy et al. 2001] D. N. McIlroy, D. Zhang, Y. Kranov, and M. G. Norton, "Nanosprings", *Appl. Phys. Lett.* **79**:10 (2001), 1540–1542.

[Mindlin 1963] R. D. Mindlin, "Influence of couple-stresses on stress concentrations", *Exp. Mech.* **3** (1963), 1–7.

[Mindlin 1964] R. D. Mindlin, "Micro-structure in linear elasticity", *Arch. Ration. Mech. Anal.* **16** (1964), 51–78.

[Mindlin and Eshel 1968] R. D. Mindlin and N. N. Eshel, "On first strain-gradient theories in linear elasticity", *Int. J. Solids Struct.* **4**:1 (1968), 109–124.

[Norouzzadeh et al. 2018a] A. Norouzzadeh, R. Ansari, and H. Rouhi, "Isogeometric vibration analysis of small-scale Timoshenko beams based on the most comprehensive size-dependent theory", *Sci. Iran.* **25**:3 (2018), 1864–1878.

[Norouzzadeh et al. 2018b] A. Norouzzadeh, R. Ansari, and H. Rouhi, "Nonlinear wave propagation analysis in Timoshenko nano-beams considering nonlocal and strain gradient effects", *Meccanica* **53** (2018), 3415–3435.

[Papargyri-Beskou and Beskos 2008] S. Papargyri-Beskou and D. E. Beskos, "Static, stability and dynamic analysis of gradient elastic flexural Kirchhoff plates", *Arch. Appl. Mech.* **78** (2008), 625–635.

[Papargyri-Beskou and Beskos 2009] S. Papargyri-Beskou and D. E. Beskos, "Stability analysis of gradient elastic circular cylindrical thin shells", *Int. J. Eng. Sci.* **47**:11-12 (2009), 1379–1385.

[Papargyri-Beskou et al. 2003] S. Papargyri-Beskou, K. G. Tsepoura, D. Polyzos, and D. E. Beskos, "Bending and stability analysis of gradient elastic beams", *Int. J. Solids Struct.* **40**:2 (2003), 385–400.

[Park and Gao 2008] S. K. Park and X.-L. Gao, "Variational formulation of a modified couple stress theory and its application to a simple shear problem", *Z. Angew. Math. Phys.* **59** (2008), 904–917.

[Polizzotto 2003] C. Polizzotto, "Gradient elasticity and nonstandard boundary conditions", *Int. J. Solids Struct.* **40**:26 (2003), 7399–7423.

[Polizzotto 2012] C. Polizzotto, "A gradient elasticity theory for second-grade materials and higher order inertia", *Int. J. Solids Struct.* **49**:15-16 (2012), 2121–2137.

[Polizzotto 2017] C. Polizzotto, "A hierarchy of simplified constitutive models within isotropic strain gradient elasticity", *Eur. J. Mech. A Solids* **61** (2017), 92–109.

[Reddy 2002] J. N. Reddy, *Energy principles and variational methods in applied mechanics*, 2nd ed., John Wiley & Sons, Hoboken, New Jersey, 2002.

[Seto et al. 2001] M. W. Seto, B. Dick, and M. J. Brett, "Microsprings and microcantilevers: studies of mechanical response", *J. Micromech. Microeng.* **11**:5 (2001), 582–588.

[Steigmann 2012] D. J. Steigmann, "Theory of elastic solids reinforced with fibers resistant to extension, flexure and twist", *Int. J. Non-Linear Mech.* **47**:7 (2012), 734–742.

[Wang et al. 2010] J.-S. Wang, Y.-H. Cui, X.-Q. Feng, G.-F. Wang, and Q.-H. Qin, "Surface effects on the elasticity of nanosprings", *Europhys. Lett.* **92**:1 (2010), 16002.

[Westcott et al. 1995] T. P. Westcott, I. Tobias, and W. K. Olson, "Elasticity theory and numerical analysis of DNA supercoiling: an application to DNA looping", *J. Phys. Chem.* **99**:51 (1995), 17926–17935.

[Yang et al. 2002] F. Yang, A. C. M. Chong, D. C. C. Lam, and P. Tong, "Couple stress based strain gradient theory for elasticity", *Int. J. Solids Struct.* **39**:10 (2002), 2731–2743.

[Zhang 2010] R. J. Zhang, "Size effects in Kirchhoff flexible rods", *Phys. Rev. E* **81** (2010), 056601.

[Zhang and Gao 2019] G. Y. Zhang and X.-L. Gao, "A non-classical Kirchhoff rod model based on the modified couple stress theory", *Acta Mech.* **230** (2019), 243–264.

[Zhu and Li 2017] X. Zhu and L. Li, "Longitudinal and torsional vibrations of size-dependent rods via nonlocal integral elasticity", *Int. J. Mech. Sci.* **133** (2017), 639–650.

Received 16 Jul 2019. Revised 6 Jan 2020. Accepted 13 Jan 2020.

JUN HONG: junhong@seu.edu.cn
Jiangsu Key Laboratory of Engineering Mechanics, School of Civil Engineering, Southeast University, 2 Sipailou Street, Nanjing, 210096, China

GONGYE ZHANG: gyzhang@seu.edu.cn
Jiangsu Key Laboratory of Engineering Mechanics, School of Civil Engineering, Southeast University, 2 Sipailou Street, Nanjing, 210096, China

XIAO WANG: xiao.wang@seu.edu.cn
Jiangsu Key Laboratory of Engineering Mechanics, School of Civil Engineering, Southeast University, 2 Sipailou Street, Nanjing, 210096, China

CHANGWEN MI: mi@seu.edu.cn
Jiangsu Key Laboratory of Engineering Mechanics, School of Civil Engineering, Southeast University, 2 Sipailou Street, Nanjing, 210096, China

JOURNAL OF MECHANICS OF MATERIALS AND STRUCTURES

msp.org/jomms

Founded by Charles R. Steele and Marie-Louise Steele

Cover photo: Mando Gomez, www.mandolux.com

See msp.org/jomms for submission guidelines.

JoMMS (ISSN 1559-3959) at Mathematical Sciences Publishers, 798 Evans Hall #6840, c/o University of California, Berkeley, CA 94720-3840, is published in 10 issues a year. The subscription price for 2020 is US $660/year for the electronic version, and $830/year (+$60, if shipping outside the US) for print and electronic. Subscriptions, requests for back issues, and changes of address should be sent to MSP.

JoMMS peer-review and production is managed by EditFLOW® from Mathematical Sciences Publishers.

PUBLISHED BY

mathematical sciences publishers

nonprofit scientific publishing

http://msp.org/

Journal of Mechanics of Materials and Structures

Volume 15, No. 2 March 2020